Available online at www.sciencedirect.com

ScienceDirect

journal homepage: www.elsevier.com/locate/he

Performance analysis of vapor-cooled shield insulation integrated with para-ortho hydrogen conversion for liquid hydrogen tanks

Chaoyue Shi [a,b,c], *Shaolong Zhu* [a,b,c], *Chuancong Wan* [a,b,c], *Shiran Bao* [a,b,c], *Xiaoqin Zhi* [a,b,c], *Limin Qiu* [a,b,c], *Kai Wang* [a,b,c,*]

[a] *Institute of Refrigeration and Cryogenics, Zhejiang University, Hangzhou 310027, China*
[b] *Key Laboratory of Refrigeration and Cryogenic Technology of Zhejiang Province, Hangzhou 310027, China*
[c] *Jiaxing Research Institute, Zhejiang University, Jiaxing 314031, China*

HIGHLIGHTS

- A composite system with VDMLI and VCS integrated with P-O conversion is proposed.
- Maximum drop of the heat leak with VCS reaches 79.9% compared to that without VCS.
- Heat leak with one VCS and catalysts is 11.6% lower than that without catalysts.
- Effect of P-O conversion efficiency on the insulation performance is explored.
- A unified criterion to evaluate the improvement of VCS number is proposed.

GRAPHICAL ABSTRACT

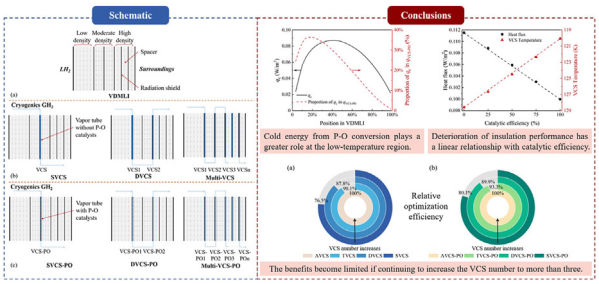

ARTICLE INFO

Article history:
Received 28 June 2022
Received in revised form
2 October 2022
Accepted 16 October 2022
Available online xxx

Keywords:
Liquid hydrogen
Multi-layer insulation
Vapor-cooled shield (VCS)

ABSTRACT

A composite thermal insulation system consisting of variable-density multi-layer insulation (VDMLI) and vapor-cooled shields (VCS) integrated with para-ortho hydrogen (P-O) conversion is proposed for long-term storage of liquid hydrogen. High-performance thermal insulation is realized by minimizing the thermal losses via the VDMLI design and fully recovering the cold energy released from the sensible heat and P-O conversion of the vented gas. Effects of different design considerations on the thermal insulation performance are studied. The results show that the maximum reduction of the heat leak with multiple VCSs can reach 79.9% compared to that without VCS. The heat leak with one VCS is reduced by 61.1%, and further reduced by 11.6% after adding catalysts. It is found that the deterioration of the insulation performance has an almost linear relationship with catalytic

* *Corresponding author*. Institute of Refrigeration and Cryogenics, Zhejiang University, Hangzhou 310027, China.
E-mail address: kaiwang19@zju.edu.cn (K. Wang).

https://doi.org/10.1016/j.ijhydene.2022.10.154

Please cite this article as: Shi C et al., Performance analysis of vapor-cooled shield insulation integrated with para-ortho hydrogen conversion for liquid hydrogen tanks, International Journal of Hydrogen Energy, https://doi.org/10.1016/j.ijhydene.2022.10.154

Para-ortho hydrogen conversion
Thermal insulation

efficiency. A unified criterion with relative optimization efficiency is finally proposed to evaluate the improvement of the VCS number.

Nomenclature

C	empirical constant
D	thickness, m
f	relative density
h	enthalpy, J/kg
k	thermal conductivity, W/(m·K)
$\dot{m}$	mass flow, kg/s
M	molecular weight, kg/mol
P	pressure, Pa
q	heat flux, W/m^2
R	universal gas constant
ROE	relative optimization efficiency
T	temperature, K

Greek letters

σ	Stefan-Boltzman constant, W/(m^2·K^4)
ε	emissivity
α	accommodation coefficient
γ	specific heat ratio
η	heat leak reduction ratio

Subscripts and superscripts

c	conversion heat
gcond	residual gas conduction
i	layer number i
in	inlet
o	orthohydrogen
out	outlet
p	parahydrogen
rad	radiation
s	sensible heat
scond	solid heat conduction
VCS	vapor-cooled shield
VCS-PO	vapor-cooled shield with catalysts

Introduction

Hydrogen is considered as one of the most promising future energy carriers due to its noteworthy advantages of renewable, environmentally friendly and high calorific value [1, 2]. However, the low density of hydrogen makes its storage an urgent technical problem for hydrogen energy development [3]. Compared with the density of gas hydrogen at 90 MPa, which is only 46.1 kg/m^3, the density of liquid hydrogen is more than 1.5 times higher, reaching 71 kg/m^3. Liquid hydrogen is thus more advantageous for large-scale storage and transportation. However, due to the large difference between the liquid hydrogen temperature and the environment temperature, an inevitable heat leak into the storage tanks of liquid hydrogen occurs, causing boil-off losses and vent of hydrogen gas. High-performance thermal insulation is crucial for long-term storage of liquid hydrogen, and further improving its performance is a long-standing challenge.

Multi-layer insulation (MLI) in high vacuum is one of the most effective cryogenic insulation methods, which is composed of radiation shields with low emissivity and spacers with low thermal conductivity. According to previous study [4], it was found that the heat transfer in MLI is dominated by the solid heat conduction near the cold boundary and the radiation heat transfer near the warm boundary. Therefore, the insulation performance can be further improved when reducing the layer density in the low-temperature region and correspondingly increasing the density in the high-temperature region, which is the so-called variable-density multi-layer insulation (VDMLI). Hedayat et al. [5, 6] proposed a VDMLI model, which divided the MLI into three parts with layer densities of 8, 12 and 16 layers/cm. The performance of the VDMLI was evaluated on NASA's Multi-purpose Hydrogen Test Bed (MHTB). It was found that the variable density contributes to a weight reduction and performance improvement. The evaporation loss with the VDMLI was reduced by 58% compared to that with standard MLI under the constant blanket weight.

Although the VDMLI reduces the heat leak to the stored liquid hydrogen, the heat leak is still unavoidable and liquid hydrogen evaporates continuously. When the liquid hydrogen tank reaches the upper limit of pressure, cryogenic hydrogen vapor accumulated in the tank needs to be vented. If a vapor-cooled shield (VCS) is placed in-between MLI layers to recover the sensible heat of vented hydrogen vapor, the performance of the thermal insulation system can be further improved.

Scott [7] first proposed the concept of VCS and carried out the theoretical analysis on the cold energy utilization of vented cryogenic vapor. The study showed that for liquid hydrogen vessels, the evaporation rate of the shielded vessel is only about 38% of the unshielded one. Bejan [8] put forward a thermodynamic method to optimize the thermal insulation system based on minimizing thermodynamic irreversibility, pointing out that the optimization of a thermal insulation system is not confined to only the reduction of the thermal conductance, but equally important to cool the insulation at intermediate temperatures. On the basis of Bejan's work, Cunnington [9] established an entropy production minimization model according to the second law of thermodynamics to minimize the evaporation rate of a thermal insulation system. He concluded that a single VCS is unable to make full use of the sensible heat of vented cryogenic hydrogen vapor, and two VCSs are more effective than one. Chato et al. [10] optimized the performance of VCSs in the MLI using a simpler method which was similar to that of Cunnington. The results showed that the maximum number of VCSs adopted in practical applications is three, and VCSs are useful only at low ratios of

Please cite this article as: Shi C et al., Performance analysis of vapor-cooled shield insulation integrated with para-ortho hydrogen conversion for liquid hydrogen tanks, International Journal of Hydrogen Energy, https://doi.org/10.1016/j.ijhydene.2022.10.154

cold boundary temperature to warm boundary temperature. Kim et al. [11] used one-dimensional thermal analysis to evaluate the composite insulation of MLI and VCS. Their results showed that for double-VCS (DVCS), the insulation performance of serial-type DVCS (the vented cryogenic hydrogen vapor passing through two VCSs sequentially) is better than that of parallel-type DVCS (the vented cryogenic hydrogen vapor passing through two parallel VCSs). In Babac et al.'s study [12], it was found that there was no difference between DVCS and single-VCS (SVCS) in the insulation effect, which was contradictory to the conclusion of Cunnington [9]. Jiang et al. [13] proposed a composite insulation system consisting of foam, VDMLI and VCS, and evaluated the contribution of the VCS in reducing the heat flux entering the cryogenic tank. They found that the VCS is particularly suitable for LH_2 storage applications compared to the liquid nitrogen (LN_2), liquid oxygen (LO_2) and liquid methane (LCH_4) storage. Zheng et al. [14] investigated the optimal position of VCS with MLI in LH_2 tanks. It showed that the maximum decrease of the heat leak is 50.16% with SVCS and 59.44% with DVCS, compared with that without VCS.

In recent years, extensive studies have been done on MLI or VDMLI coupled with multi-VCS, but the conclusions are not always consistent. For example, some studies claimed that two or even three VCSs are more effective on the insulation performance, while other studies concluded that there is little improvement with multiple VCSs. The inconsistent findings are attributed to the lack of a uniform criterion for evaluating the impact of VCS number. Existing studies only pointed out that the insulation performance can be improved with the increase of VCS number but the magnitude of improvement decreases continuously. Different from previous investigations, the present study assesses the impact of VCS number with the reference to the theoretical limit of the system with VCS.

Although VDMLI coupled with VCS significantly improves the thermal insulation performance, pursing even better insulation performance is always desirable in practical applications. Compared with other cryogens, hydrogen has a unique feature that it is a mixture of two spin isomers in nature, namely orthohydrogen (o-H_2) and parahydrogen (p-H_2). The two protons spin in the same direction for orthohydrogen, while they are in the opposite direction for parahydrogen. As parahydrogen has a lower internal energy than orthohydrogen, the conversion of ortho-para hydrogen (O-P) is an exothermic process, while the reverse reaction, i.e., the conversion process from parahydrogen to orthohydrogen (P-O), is endothermic. Meanwhile, the equilibrium concentration of orthohydrogen and parahydrogen is a function of temperature [15]. The normal hydrogen, which is in the equilibrium state at room temperature, consists of 75% orthohydrogen and 25% parahydrogen. At the normal boiling point, the composition becomes 0.2% orthohydrogen and 99.8% parahydrogen. In the process of hydrogen liquefaction, O-P conversion is a crucial step [16–19]. If hydrogen is stored mostly in the form of orthohydrogen, it can cause unacceptable boil-off loss in the liquid hydrogen tank due to the large amount of heat released from the spontaneous O-P conversion. Catalysts are usually used in the liquefaction process to speed up the conversion to ensure the liquid hydrogen product is mostly parahydrogen. When cryogenic hydrogen gas in a liquid hydrogen tank is vented, the parahydrogen concentration of the vented hydrogen is still high due to the slow spontaneous conversion rate. Therefore, in addition to the sensible heat, a large amount of P-O conversion heat (i.e., cold energy) can be utilized. If this extra cold energy can be utilized appropriately, the performance of thermal insulation can be further improved.

Up to now, only a limited number of studies have been done on the utilization of cold energy of P-O conversion. Lockheed company [20] experimentally verified the feasibility of using hydrogen vapor coupled catalytic conversion of P-O for cooling sensors and instruments. Bliesner et al. [21] and Pedrow et al. [22] explored the improvement of cooling capacity of VCS by P-O conversion during long-duration storage of LH_2 and LO_2 rocket propellants. The experimental results showed that the insulation system was greatly improved after adding catalysts. Wang et al. [23] proposed four schemes for the utilization of cold energy released by P-O conversion in deep space exploration applications. The results showed that the continuous conversion can make full use of cold energy compared with the adiabatic conversion and isothermal conversion. Existing studies have experimentally verified the feasibility of utilizing the cold energy of P-O conversion to enhance thermal insulation performance in various applications. However, few studies have explored the potential of P-O conversion combined with VCS for improving insulation performance. It is believed that an integrated theoretical model with VDMLI, VCS and P-O conversion will be conducive to a more comprehensive understanding of the influence mechanism of P-O conversion on the composite insulation system.

This paper presents a thermodynamic model of the composite insulation system for LH_2 tank to investigate the insulation performance of VDMLI with multi-VCS integrated with P-O conversion. The model is validated against experimental data of LH_2 and LN_2 storage tanks. Subsequently, the heat leaks in different design schemes are obtained, and the heat fluxes and the temperature profiles of the systems with different VCS number are investigated. The influence mechanism of P-O conversion on the composite insulation system is quantitatively analyzed, and the optimal position of VCS and the change of the heat flux with or without P-O conversion are compared. The effect of catalytic efficiency on the insulation performance is then analyzed. Finally, a unified evaluation criterion is proposed to evaluate the improvement of thermal insulation performance of liquid hydrogen storage tank with various thermal insulation techniques.

Thermodynamic model and validation

Physical model

Fig. 1 shows the configurations of the composite insulation system for LH_2 tanks. Based on the baseline case with a VDMLI shown in Fig. 1(a), the case shown in Fig. 1(b) adds multiple VCSs, while the case shown in Fig. 1(c) adds P-O catalysts in the vapor tube correspondingly. In order to explore the effect of the VCS number and P-O conversion on the insulation performance of the VDMLI system, a thermodynamic modelling framework is established. The main parameters of the VDMLI are selected the same as those in the MHTB [24], as shown in

Please cite this article as: Shi C et al., Performance analysis of vapor-cooled shield insulation integrated with para-ortho hydrogen conversion for liquid hydrogen tanks, International Journal of Hydrogen Energy, https://doi.org/10.1016/j.ijhydene.2022.10.154

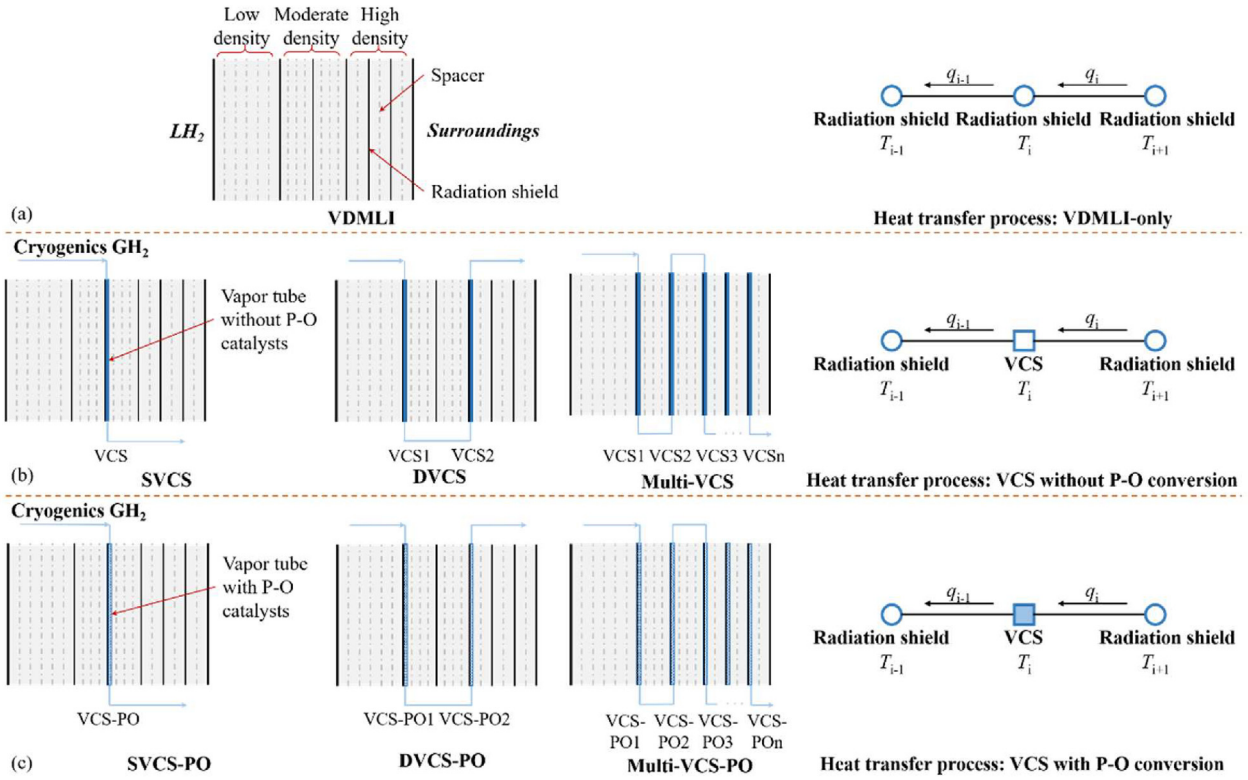

Fig. 1 – Schematic of various thermal insulation systems and heat transfer processes: (a) VDMLI-only, (b) VCS without P-O conversion and (c) VCS with P-O conversion.

Table 1, because the thermal insulation performance has been verified in liquid hydrogen experiments, and several other studies also adopted the same arrangement [25]. The VDMLI is composed of three segments with the same thickness and different layer densities, i.e., the density reduces from the cold side to the ambient side. Aluminum foil and Dacron net are chosen as the materials of radiation shield and spacer, respectively, same as the materials used in the MTHB [24].

The VCS is composed of a cryogenic hydrogen vapor tube and adjacent radiation shield which are in good thermal contact with each other. When the number of the VCS exceeds one, the performance of serial-type is superior to parallel-type according to the previous research [11]. Therefore, multiple VCSs are arranged in the form of serial-type. When the maximum number of VCSs is equal to the number of radiation shield layers, i.e., all shields are cooled by vented vapor, the case is named as All-VCS (AVCS).

For the cases with the P-O conversion, para-ortho hydrogen catalysts are filled in the vapor tube uniformly to ensure the sufficient conversion of hydrogen. Iron-based catalysts are used in this model, which are often used for the ortho-para hydrogen conversion in hydrogen liquefiers [17, 26]. However, owing to the lack of relevant studies on the reaction kinetics of P-O conversion, the catalytic efficiency is set to ideal 100% in this paper.

Table 1 – Main parameters of VDMLI.

Parameters	Value
Low-density layers	8 layers/cm (1.25 cm)
Moderate-density layers	12 layers/cm (1.25 cm)
High-density layers	16 layers/cm (1.25 cm)
Total number of layers	45
Total thickness	3.75 cm
Materials	Aluminum foil & Dacron net

Assumptions

To simplify the calculations, the following assumptions are made:

(1) The LH_2 tank and composite insulation system are assumed to be in steady state;
(2) The jacket of the LH_2 tank is maintained in high vacuum (5×10^{-3} Pa), and the surroundings temperature is maintained at 300 K;
(3) LH_2 in the tank is maintained at 0.1 MPa and 20 K, and the temperature of the tank wall is equal to the LH_2 temperature;
(4) Thermal resistance of the tank wall can be ignored;
(5) The VCS temperature is assumed to be equal to the adjacent MLI layer and the temperature is uniform throughout the VCS;
(6) Flow resistance of catalysts in the VCS tube can be ignored.
(7) Hydrogen is in full contact with the catalysts in the VCS tube and parahydrogen is converted to the equilibrium concentration at the VCS-PO temperature after flowing through the VCS-PO, that is, the catalytic efficiency is 100%.

Please cite this article as: Shi C et al., Performance analysis of vapor-cooled shield insulation integrated with para-ortho hydrogen conversion for liquid hydrogen tanks, International Journal of Hydrogen Energy, https://doi.org/10.1016/j.ijhydene.2022.10.154

Heat transfer model of VDMLI

There are mainly two models to calculate the MLI performance: the layer-by-layer model [27] and Lockheed model [28]. For the convenience of obtaining the temperature distribution and the heat flux in the MLI, the layer-by-layer model is selected here. The layer-by-layer model is based on an iterative algorithm, proposed by McIntosh [27]. The heat transfer between adjacent radiation shields is divided into three parts: radiation heat transfer, solid heat conduction and residual gas conduction, as given in Eq. (1).

$$q^{i} = q^{i}_{rad} + q^{i}_{scond} + q^{i}_{gcond} \tag{1}$$

The radiation heat transfer is written as [29].

$$q^{i}_{rad} = \frac{\sigma\left(T^{4}_{i+1} - T^{4}_{i}\right)}{\left({}^{1}/_{\varepsilon_{i+1}} + {}^{1}/_{\varepsilon_{i}} - 1\right)} \tag{2}$$

where σ is the Stefan-Boltzman constant, 5.67×10^{-8} W/($m^2 \cdot K^4$); T_{i+1} and T_i are the temperature of the outer and inner radiation shields, respectively; ε_{i+1} and ε_i are the emissivity of the outer and inner radiation shields, respectively.

The solid conduction between adjacent radiation shields is written as [29].

$$q^{i}_{scond} = \frac{C_1 f k}{D_x}\left(T_{i+1} - T_i\right) \tag{3}$$

where C_1 is an empirical constant, set as 0.016 [30]; f is the relative density of spacer material and solid material; D_x is the actual thickness between adjacent radiation shields, which varies with layer density; k is the thermal conductivity of spacer material, calculated by Eq. (4) [27]:

$$k = 0.017 + 7 \times 10^{-6}(800 - T) + 0.228 \ln(T) \tag{4}$$

The gas conduction is written as [31]

$$q^{i}_{gcond} = C_2 P \alpha (T_{i+1} - T_i) \tag{5}$$

where P is the residual gas pressure; α is the accommodation coefficient, which is 0.9 for air. C_2 is an empirical constant, calculated by the following expression:

$$C_2 = \frac{\gamma + 1}{\gamma - 1}\sqrt{\frac{R}{8\pi M T}} \tag{6}$$

where γ is the specific heat ratio, R is the universal gas constant and M is the molecular weight of gas. For the case where the residual gas is air and the warm boundary temperature is room temperature, $C_2 = 1.1666$.

VCS model with/without P-O conversion

Fig. 1 also shows the schematics of the heat transfer processes for different cases. For the VDMLI-only case, the heat flux between each two radiation shields is equal at steady state (see Fig. 1(a)), which can be expressed as follows:

$$q_i = q_{i-1} \tag{7}$$

For the VDMLI coupled with VCS only, part of the total heat leak from the external environment is absorbed by the VCS in terms of the sensible heat of the vented cryogenic hydrogen gas, and the remaining passes through the VCS and reaches the tank, as shown in Fig. 1(b). According to the conservation of energy, the heat flux of the VDMLI with VCS is expressed as:

$$q_i = q_{VCS} + q_{i-1} \tag{8}$$

where q_{VCS} is the sensible heat recovered by the VCS, calculated by

$$q_{VCS} = \dot{m}\Delta h_{VCS} = \dot{m}\left(h_{out,p} - h_{in,p}\right) \tag{9}$$

where $\dot{m}$ is the mass flow of vented hydrogen gas, $h_{out,p}$ and $h_{in,p}$ are the enthalpy of parahydrogen at the outlet temperature and the inlet temperature of VCS, respectively.

For the VDMLI coupled with VCS and P-O conversion, compared with the case with VCS only, the VCS-PO can recover the cold energy arising from not only the sensible heat, but also the P-O conversion, as illustrated in Fig. 1(c). The heat flux of the VDMLI with VCS and P-O conversion is expressed as follows:

$$q_i = q_{VCS-PO} + q_{i-1} \tag{10}$$

$$q_{VCS-PO} = \dot{m}\Delta h_{VCS-PO} = \dot{m}\left(\left(h_{out,p}x_{out,p} + h_{out,o}\left(1 - x_{out,p}\right)\right.\right. \times \left.\left.\right) - \left(h_{in,p}x_{in,p} + h_{in,o}\left(1 - x_{in,p}\right)\right)\right) \tag{11}$$

where $h_{out,o}$ and $h_{in,o}$ are the enthalpy of orthohydrogen at the outlet and inlet of the VCS, respectively; $x_{out,p}$ and $x_{in,p}$ are the equilibrium concentration of parahydrogen at the outlet and inlet of the VCS, respectively.

In order to study the effect of P-O conversion on the insulation performance, the heat taken away by the VCS-PO, q_{VCS-PO}, is divided into two parts: the heat taken away by the sensible heat, q_s, and the heat taken away by the conversion heat, q_c, which are expressed as follows:

$$q_{VCS-PO} = q_s + q_c \tag{12}$$

$$q_s = \dot{m}\left(\left(h_{out,p}x_{in,p} + h_{out,o}\left(1 - x_{in,p}\right)\right) - \left(h_{in,p}x_{in,p} + h_{in,o}\left(1 - x_{in,p}\right)\right)\right) \tag{13}$$

$$q_c = \dot{m}\left(\left(h_{out,p}x_{out,p} + h_{out,o}\left(1 - x_{out,p}\right)\right.\right. \times \left.\left.\right) - \left(h_{out,p}x_{in,p} + h_{out,o}\left(1 - x_{in,p}\right)\right)\right) \tag{14}$$

Model verification

Three sets of experimental data of VDMLI from Martin et al. [24], Wang et al. [32] and Huang et al. [33] are used to validate the proposed model. The results of the temperature profile and heat flux are shown in Fig. 2. It is observed that the trends obtained from simulations agree well with the experiments. The average deviations of the temperature profile inside the insulation structure between the simulation and experiment are 7.5%, 6.0% and 0.9% for the three sets of data, respectively. The average deviations of the heat leak are 12.7% and 7.6%, respectively. The deviation mainly exists near the cold boundary, as it is difficult to reach the high vacuum condition there, resulting in a faster temperature rise in practice. Overall, the simulated temperature profile and heat flux are in good agreement with the experimental results. Thus, the

Please cite this article as: Shi C et al., Performance analysis of vapor-cooled shield insulation integrated with para-ortho hydrogen conversion for liquid hydrogen tanks, International Journal of Hydrogen Energy, https://doi.org/10.1016/j.ijhydene.2022.10.154

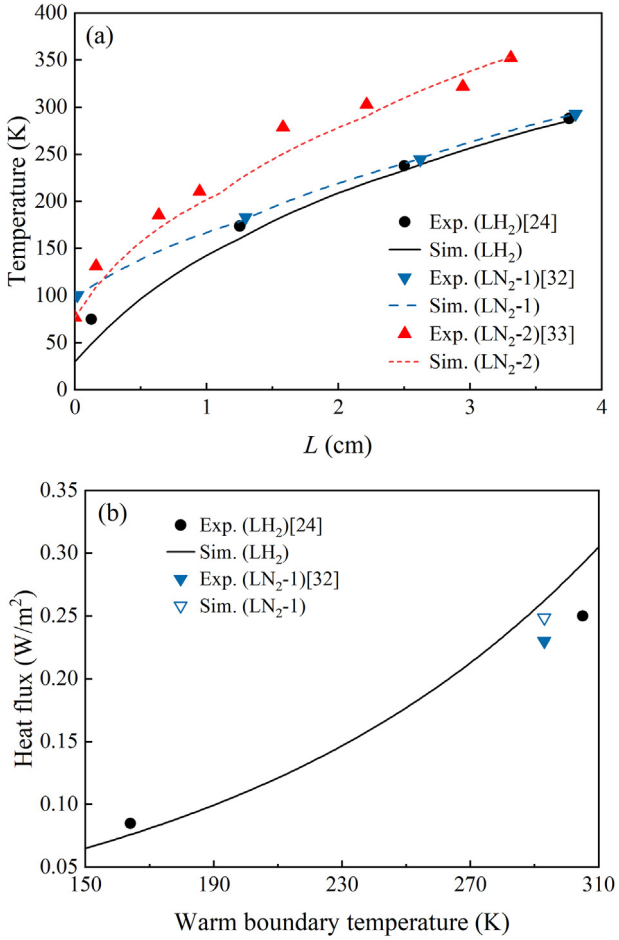

Fig. 2 – Comparison between experiments and simulations for (a) temperature profile and (b) heat flux.

model has a reasonable accuracy for predicting the insulation performance of VDMLI coupled with VCS and P-O conversion.

Results and discussion

Effect of VCS number

In order to explore the improvement of insulation performance of composite system insulation system by increasing the number of VCS, the insulation performance comparison of different VCS number is shown in Table 2. For the AVCS case, each radiation layer is cooled by the vented cold hydrogen gas, so that the sensible heat (cold energy) can be utilized entirely. Therefore, it is the optimal case for the VDMLI with multi-VCS. It can be observed that with the increase of the VCS number, the actual heat flux into the tank decreases due to the increase in the heat taken away by the VCS, although the total heat flux at the optimal positions of the VCSs gradually increases. Compared with the heat leak of 0.288 W/m^2 for the non-VCS case, the heat leak can be reduced by 61.1%, 70.1% and 73.6% for the SVCS, DVCS and triple-VCS (TVCS) cases, respectively. The maximum reduction reaches 79.9% for the most idealized case, when all layers of insulation are coupled with VCSs, i.e., the AVCS case. This is also the theoretical limit of the performance improvement that can be achieved by this VDMLI arrangement with multi-VCS.

Table 2 – Comparisons of insulation performance for different VCS number.

Case	Heat leak into the tank q_0 (W/m^2)	Heat taken away by VCS q_{VCS} (W/m^2)	Total heat leak q_{total} (W/m^2)
non-VCS	0.288	–	0.288
SVCS	0.112	0.326	0.438
DVCS	0.086	0.400	0.486
TVCS	0.076	0.412	0.488
AVCS	0.058	0.506	0.564

Fig. 3 shows the comparison of the proportion of the three heat transfer modes (radiation, solid heat conduction and gas

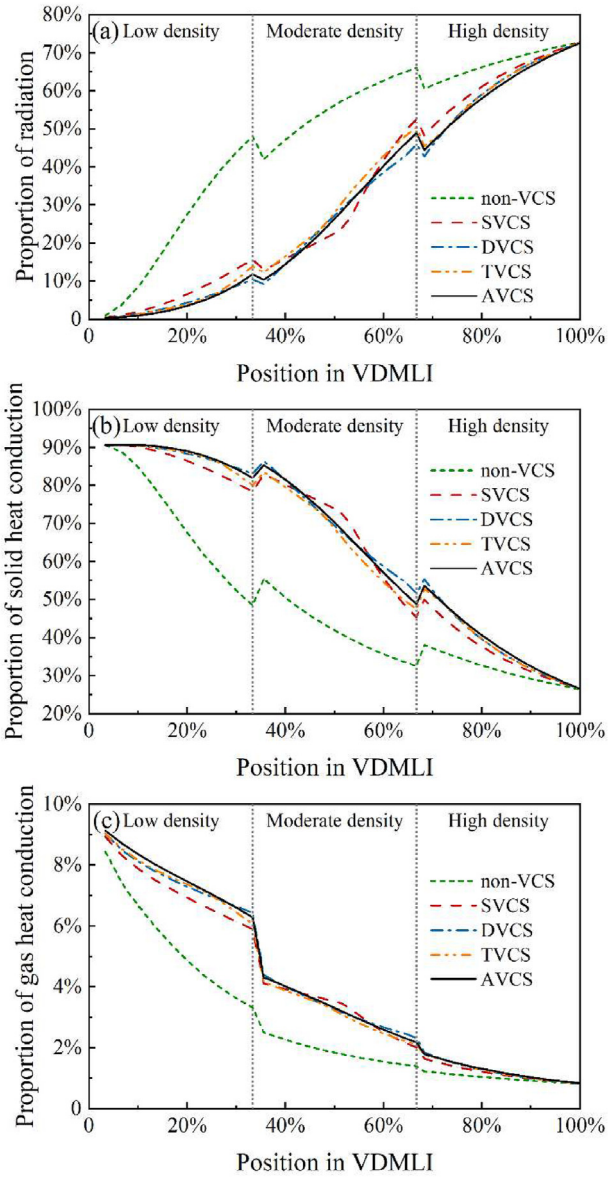

Fig. 3 – Comparison of proportion of three heat transfer modes with different number of VCS: (a) radiation, (b) solid heat conduction and (c) gas heat conduction.

Please cite this article as: Shi C et al., Performance analysis of vapor-cooled shield insulation integrated with para-ortho hydrogen conversion for liquid hydrogen tanks, International Journal of Hydrogen Energy, https://doi.org/10.1016/j.ijhydene.2022.10.154

heat conduction) with different VCS number. Note that 0% stands for the cold boundary of VDMLI and the warm boundary corresponds to the position 100%. After adding VCS, the proportion of radiation is significantly reduced, while the proportion of solid heat conduction and gas heat conduction is increased. The change trends of the proportion under different number of VCSs are similar. When the number of VCS exceeds two, the change of proportion is almost identical. The proportion of radiation increases along the direction from the cold to warm boundary in the VDMLI. In the absence of VCS, the proportion of radiation increases rapidly in the low-density region of the VDMLI, i.e., the region adjacent to the liquid hydrogen tank wall, while the growth rate slows down gradually in the moderate-density and high-density regions. When adding VCS, the growth rate of radiation proportion in the low-density region slows down obviously, while those in the moderate-density and high-density regions are faster. However, the proportion of solid heat conduction and gas heat conduction has a similar declining trend, which is opposite to that of radiation. For the heat conduction losses, the proportion in the low-density region decreases rapidly for the non-VCS case, and then the declining rate gradually slows down. After adding VCS, however, the heat conduction losses decrease slowly in the low-density region, and then the declining rate increases in the high-temperature regions.

Fig. 4 illustrates the temperature profiles in the VDMLI with different number of VCS. It is observed that adding the VCS significantly affects the temperature profile in the VDMLI. For the non-VCS case, as more spacers are placed near the cold boundary, a larger temperature difference between adjacent radiation shields makes the temperature rise faster. The addition of VCS expands the low-temperature region in the VDMLI, which makes up for the problem of the thin low-temperature region in the VDMLI. Thus, the coupling optimization performance of VDMLI and VCS performs well. As the VCS number increases, the temperature profile near the tank wall becomes flatter, which implies that the heat flux into the tank decreases, but the differences are not significant using different number of VCS.

Optimization mechanism of P-O conversion

To facilitate investigating the improvement of thermal insulation performance by P-O conversion, the cases with SVCS and SVCS-PO are compared and analyzed here. Due to that placing a VCS or VCS-PO in a proper position in the VDMLI has a great impact on the performance of the composite insulation system, the effect of the position of the SVCS or SVCS-PO in the VDMLI on the heat leak is shown in Fig. 5. It can be observed that whether P-O conversion is integrated or not, the change trend of the heat leak has the same tendency for the SVCS and SVCS-PO cases, which decreases first and then increases while moving the SVCS or SVCS-PO outwards along the VDMLI. The optimum installation position of the SVCS is around 51% in the VDMLI, with the minimum heat leak into the tank of 0.112 W/m^2. When adding catalysts into the SVCS and forming the SVCS-PO, an obvious reduction of the heat leak is observed and the heat leak is lower than the lowest value of the SVCS case when the position of the VCS-PO is between 20% and 70% within the VDMLI. The optimum installation position of the VCS-PO is around 45% in the VDMLI, with the minimum heat leak into the tank of 0.099 W/m^2, which is 11.6% lower than that of the case with the SVCS. This indicates that the addition of the P-O conversion further improves the original high thermal insulation performance.

In order to investigate the mechanism of P-O conversion affecting the performance of the composite insulation system, the heat taken away by the sensible heat and the conversion heat versus the position of the SVCS or SVCS-PO is compared and analyzed, as shown in Fig. 6(a). As the SVCS and SVCS-PO move outwards along the layers of the VDMLI, the heat taken away by them both increases gradually, and the heat taken away by the SVCS is slightly less than that by the SVCS-PO. In the SVCS-PO, the heat taken away by the VCS-PO, $q_{VCS\text{-}PO}$, is equal to the sum of the heat taken away by the sensible heat, q_s, and the heat taken away by the conversion heat, q_c, as shown in Eq. (12). However, q_c increases first and then decreases gradually with the SVCS-PO moving outwards, which is different from the trend of q_s.

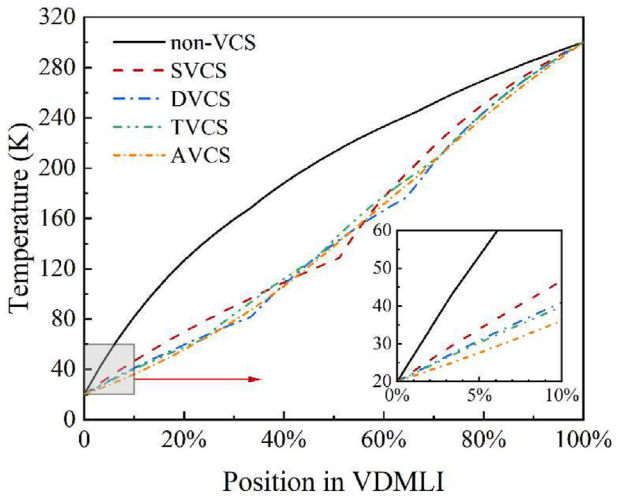

Fig. 4 – Temperature profile with different VCS number.

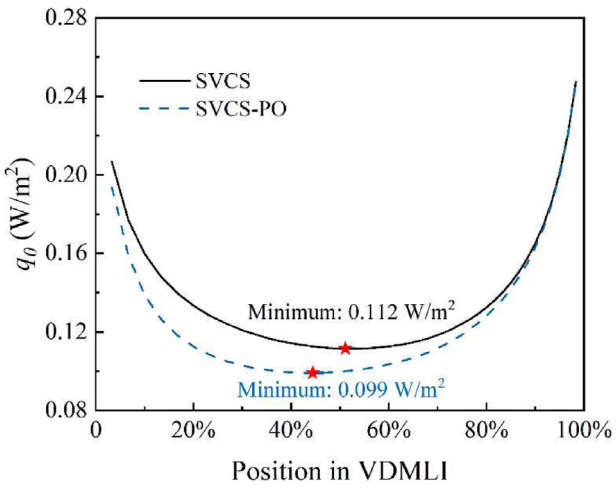

Fig. 5 – Heat leak versus position of SVCS or SVCS-PO.

Please cite this article as: Shi C et al., Performance analysis of vapor-cooled shield insulation integrated with para-ortho hydrogen conversion for liquid hydrogen tanks, International Journal of Hydrogen Energy, https://doi.org/10.1016/j.ijhydene.2022.10.154

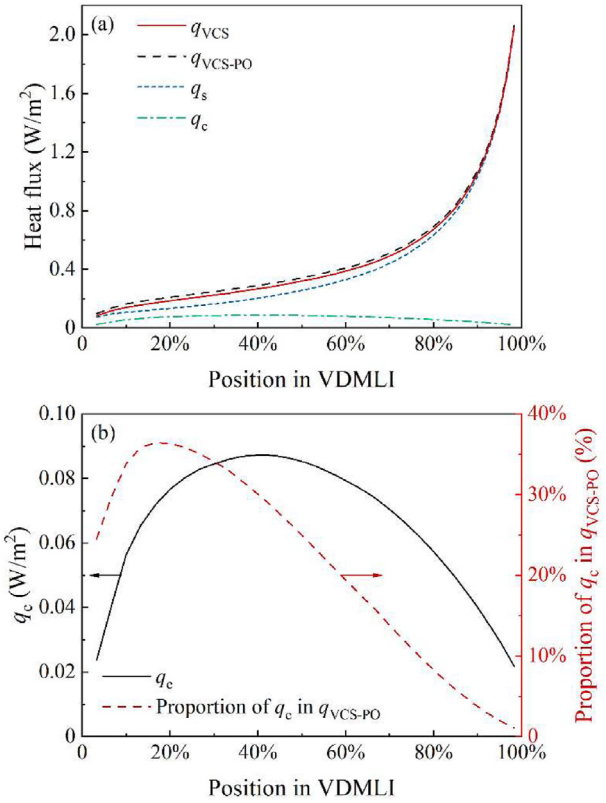

Fig. 6 – (a) Heat taken away by the sensible heat and the conversion heat versus position of SVCS or SVCS-PO and (b) heat taken away by the conversion heat q_c and its proportion in the heat taken away by VCS-PO q_{VCS-PO} versus position of SVCS-PO.

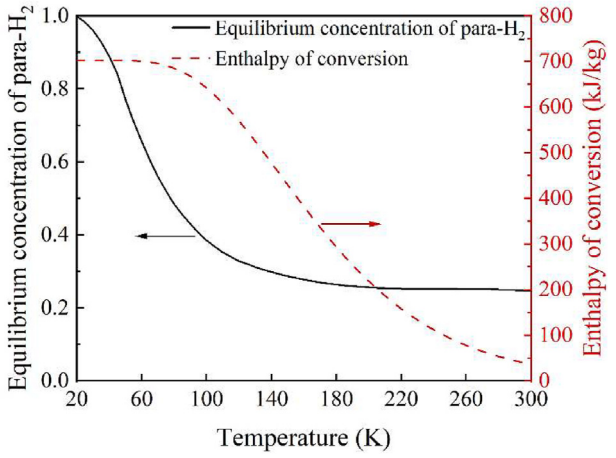

Fig. 7 – Equilibrium concentration of para-H_2 and enthalpy of conversion varying with temperature.

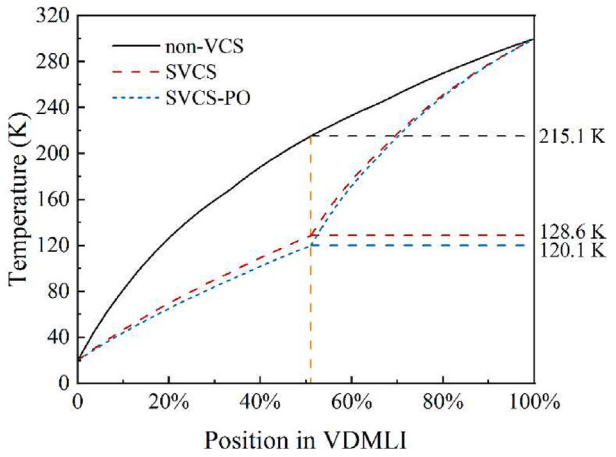

Fig. 8 – Comparison of temperature profiles of non-VCS, SVCS and SVCS-PO.

Fig. 6(b) shows the heat taken away by the conversion heat, q_c, and the proportion of q_c in q_{VCS-PO} versus the position of the SVCS-PO. It can be observed that the peak of q_c is achieved at around 40% in the VDMLI, and the peak of the proportion of q_c in q_{VCS-PO} is reached at around 16.7%, with a value of 36.5%. q_c is the product of the mass flowrate of vented hydrogen gas, concentration difference and the enthalpy of conversion, as shown in Eq. (14). The variations of parahydrogen equilibrium concentration and enthalpy of conversion with temperature are shown in Fig. 7 [34]. As the position of the SVCS-PO is moved outwards in the VDMLI, leading to an increase of the hydrogen vapor temperature, a higher parahydrogen equilibrium concentration can be reached. However, the enthalpy of conversion has an opposite trend, decreasing with increasing temperature. Hence a peak of q_c appears in the middle of the VDMLI. The optimal location of the VCS-PO is dependent on the combined optimization of the VCS and P-O conversion. Although the heat taken away by the sensible heat, q_s, is the dominant part in the heat taken away by the VCS-PO, q_{VCS-PO}, the cold energy from the P-O conversion plays a relatively greater role at the low-temperature region, i.e., closer to the tank wall.

Fig. 8 shows the comparison of temperature profiles of the non-VCS, SVCS and SVCS-PO cases. In order to illustrate the effect of the P-O conversion intuitively, the SVCS and SVCS-PO are placed at the same location of the VDMLI, i.e., 51%. When the VCS is added to the VDMLI with non-VCS, the temperature at the position where the VCS is added drops from 215.1 K to 128.6 K, and is further decreased to 120.1 K after the P-O conversion is further added. The VCS provides an internal cooling source to the VDMLI, and divides the VDMLI into two parts. The heat leak to the LH_2 tank decreases since the temperature gradient of the VDMLI layers inside the VCS is smaller than that without any VCS. Accordingly, as the temperature gradient of the VDMLI layers outside the VCS is higher for the SVCS and SVCS-PO cases comparing to the non-VCS case, an increase in the total heat flux is thus observed after adding the VCS, as presented in Table 2.

To better understand the differences of the heat transfer mechanisms between the SVCS-PO and SVCS cases, the ratios of the heat fluxes of the SVCS-PO case over that of the SVCS case are calculated and illustrated in Fig. 9. An obvious difference in the heat flux ratios is observed on the two sides of the VCS. The heat fluxes of the three heat transfer modes in the SVCS-PO case are smaller than those of the SVCS case at the inner side of the VCS, while it is opposite at the outer side. The radiation variation is remarkably different from the other two modes on account of the fact that the radiation has a fourth power relationship with temperature, as shown in Eq.

Please cite this article as: Shi C et al., Performance analysis of vapor-cooled shield insulation integrated with para-ortho hydrogen conversion for liquid hydrogen tanks, International Journal of Hydrogen Energy, https://doi.org/10.1016/j.ijhydene.2022.10.154

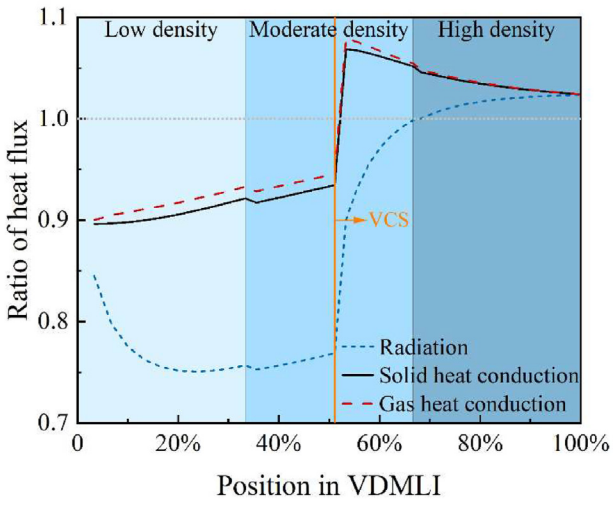

Fig. 9 – Ratio of heat fluxes of the SVCS-PO case over those of the SVCS case.

(2), while the heat conduction of solid and gas has a linear relationship with temperature, as shown in Eq. (3) and Eq. (5). Therefore, the addition of catalysts mainly affects the temperature distribution in the VDMLI as shown in Fig. 8, resulting in the variation of heat fluxes.

Performance of multi-VCS coupled with P-O conversion

The performance of the VDMLI with different configurations of multi-VCS coupled with P-O conversion is further studied. Fig. 10 shows the heat flux versus the positions of the VCS1 (inside) and VCS2 (outside) with or without P-O conversion for the cases with double VCSs (i.e., DVCS and DVCS-PO). As shown in Fig. 10(a), for the DVCS case, when the positions of the VCS1 and VCS2 are 33.3% and 64.4% in the VDMLI respectively, the heat leak into the tank is the smallest, reaching 0.086 W/m^2, with a reduction of 70.1% compared to the case without a VCS and 23.2% compared to the case with the SVCS. This implies that there is still an appreciable amount of cold energy available after cold hydrogen gas passing through one VCS. When the two VCSs are located at 20%–80% position of the VDMLI, the insulation performance is superior to that with the SVCS. The result of the DVCS-PO case in which the P-O conversion is integrated is shown in Fig. 10(b). When the positions of the VCS1 and VCS2 are 30% and 60% in the VDMLI respectively, the heat leak into the tank reaches its minimum value of 0.076 W/m^2, with a further drop of 11.6% compared to the case with the DVCS. Similar to the SVCS, the optimal positions of the two VCSs in the case with the DVCS-PO move inwards compared to the case with the DVCS. In addition, since the minimum value of the heat leak is only at one optimum point, which is not conducive to the practical applications of the DVCS and DVCS-PO, the optimal regions which provide more flexible choices for the arrangement of the DVCS and DVCS-PO are given in the contour maps, and the heat leaks in these regions are only 2.3% and 2.6% larger than the minimum values, respectively.

Fig. 11 shows the heat flux versus the position in the VDMLI with different number of VCS and with/without P-O conversion. Except for the AVCS and AVCS-PO cases, the heat taken away by the VCS or VCS-PO on the outside is greater than that on the inside regardless of whether considering P-O conversion. For the TVCS-PO case, the heat taken away by the conversion heat in the third VCS is almost negligible, as shown in Fig. 11(d). For the cases with the AVCS and AVCS-PO, the heat taken away by each VCS or VCS-PO increases first and then decreases, because the temperature difference between adjacent VCSs has the same trend, and the enthalpy of hydrogen has an almost linear relationship with temperature. In the AVCS-PO case, the heat taken away by the conversion heat can be neglected compared to that by the sensible heat at the position between 50% and 100% within the VDMLI. Table 3 shows the comparison of insulation performance of different number of the VCS-PO. As shown, the heat taken away by the sensible heat (q_s) increases gradually with the increase of the number of the installed VCSs, while the heat taken away by the conversion heat (q_c) and its proportion of the heat taken away by the VCS-PO (q_{VCS-PO}) decrease. This is due to the fact that the heat taken away by the conversion heat is dependent on not only the concentration difference, but also the enthalpy of conversion, which both vary with the temperature.

Effect of catalytic efficiency

For the aforementioned results presented in previous sections, the catalytic conversion is assumed as a perfect process

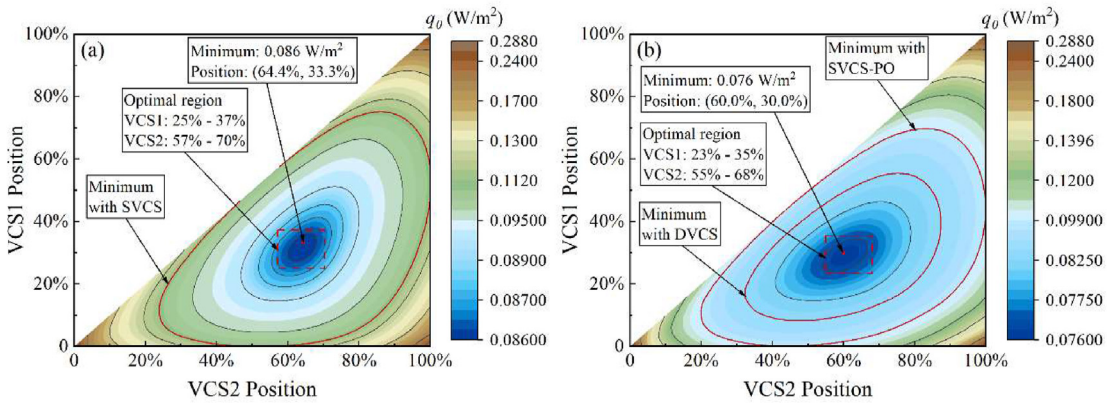

Fig. 10 – Heat flux versus position of the two VCSs for the cases of: (a) DVCS and (b) DVCS-PO.

Please cite this article as: Shi C et al., Performance analysis of vapor-cooled shield insulation integrated with para-ortho hydrogen conversion for liquid hydrogen tanks, International Journal of Hydrogen Energy, https://doi.org/10.1016/j.ijhydene.2022.10.154

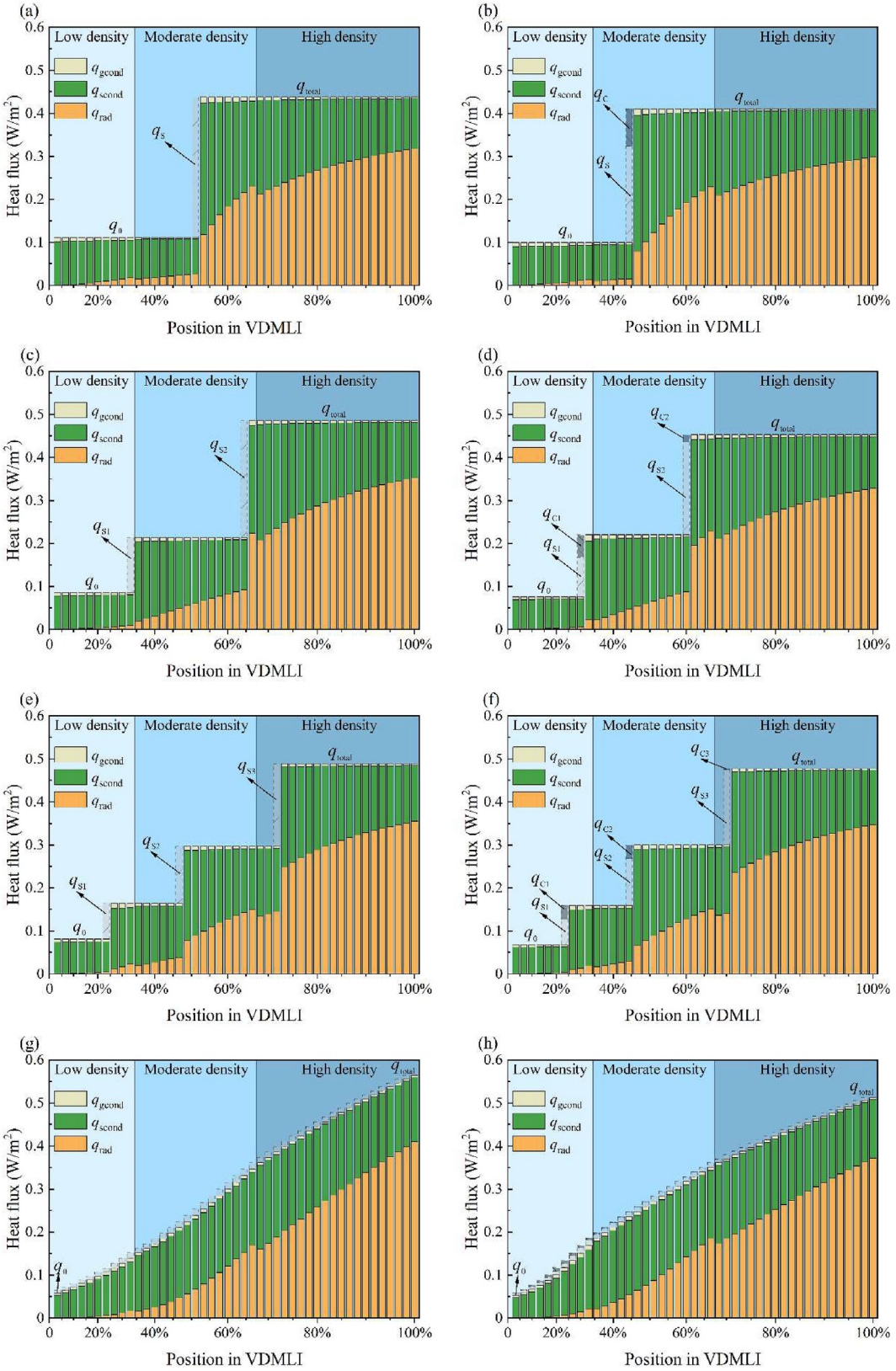

Fig. 11 – Heat flux versus position in VDMLI with (a) SVCS, (b) SVCS-PO, (c) DVCS, (d) DVCS-PO, (e) TVCS, (f) TVCS-PO, (g) AVCS, (h) AVCS-PO.

Please cite this article as: Shi C et al., Performance analysis of vapor-cooled shield insulation integrated with para-ortho hydrogen conversion for liquid hydrogen tanks, International Journal of Hydrogen Energy, https://doi.org/10.1016/j.ijhydene.2022.10.154

Table 3 – Insulation performance comparison of different VCS-PO number.

Case	Heat leak into the tank q_0 (W/m^2)	Heat taken away by VCS-PO $q_{VCS\text{-}PO}$ (W/m^2)	Heat taken away by the sensible heat q_s (W/m^2)	Heat taken away by the conversion heat q_c (W/m^2)	Proportion of heat taken away by the conversion heat $q_c/q_{VCS\text{-}PO}$ (%)	Total heat leak q_{total} (W/m^2)
SVCS-PO	0.099	0.312	0.225	0.087	27.9	0.411
DVCS-PO	0.076	0.376	0.308	0.068	18.1	0.452
TVCS-PO	0.068	0.41	0.344	0.066	16.1	0.478
AVCS-PO	0.052	0.46	0.403	0.057	10.9	0.512

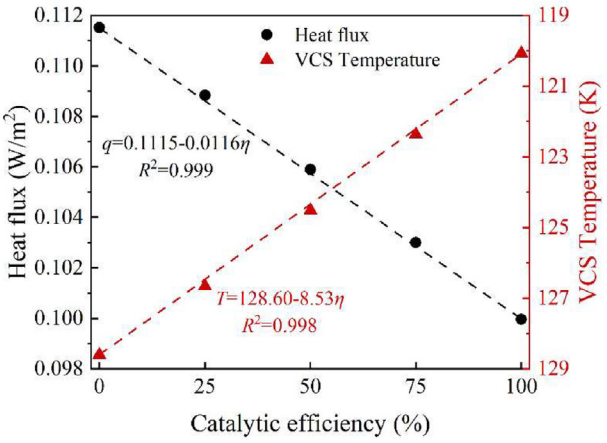

Fig. 12 – Heat flux and VCS temperature versus catalytic efficiency.

with the catalytic efficiency of 100%. However, in practice, the catalytic efficiency is affected by various factors, e.g., limited contact time, insufficient contact area, imperfect catalyst activity, etc., and thus it is always less than 100%. Here, the effect of the catalytic efficiency on the insulation performance is thus further studied. In order to observe the effect of the catalytic efficiency visually, SVCS is adopted in this session.

Fig. 12 shows the heat flux and the VCS temperature versus catalytic efficiency. 0% refers to no P-O conversion, while 100% represents complete conversion to the equilibrium state. As the catalytic efficiency decreases from 100% to 0%, the optimal position of VCS-PO gradually moves outward in the VDMLI, and the heat flux into the tank increases gradually. It is worth mentioning that the improvement of insulation performance has a linear relationship with the catalytic efficiency, with a fitting error of 0.999. Meanwhile, the VCS temperature gradually increases with the decrease of the catalytic efficiency, and the reduction magnitude is also linear with the catalytic efficiency with a fitting error of 0.998, which is attributed to the fact that the effect of the catalytic efficiency on the overall heat taken away by VCS-PO is relatively slight, as shown in Table 3.

At present, experimental data on the P-O conversion rate are lacking, making it impossible to get the actual para-hydrogen concentration after the catalytic conversion. If the catalytic efficiency data are obtained in future studies, more accurate predictions about the insulation performance improvement with P-O conversion can be attainable.

Relative optimization efficiency

For purpose of establishing a unified criteria for evaluating the improvement effect of VCS number on the thermal insulation performance, the relative optimization efficiency (*ROE*) is proposed to judge the degree of approaching the optimal insulation performance for a specific VDMLI insulation configuration, which is analogous to the relative Carnot efficiency. The calculation steps are as follows.

1) According to the given MLI/VDMLI parameters, the heat leak of the case without VCS and the ideal optimal case, that is the heat leak of the All-VCS case, are obtained.
2) The optimal heat leak reduction, $\eta_{optimal}$, compared with the case without VCS can be calculated using Eq. (15), which is only determined by given parameters. $\eta_{optimal}$ is the benchmark for *ROE* under given conditions.

$$\eta_{optimal} = \left(1 - \frac{q_{0,AVCS}}{q_{0,non-VCS}}\right) \times 100\% \quad (15)$$

3) Similar to the Step 2, the heat leak reduction, η_n, with different VCS numbers can be obtained.

$$\eta_n = \left(1 - \frac{q_{0,nVCS}}{q_{0,non-VCS}}\right) \times 100\% \quad (16)$$

4) *ROE*, that is the extent of how far the performance of the case is deviated from that of the ideal optimal case, can be obtained as follows.

$$ROE_n = \frac{\eta_n}{\eta_{optimal}} \times 100\% \quad (17)$$

Table 4 shows the comparison of *ROE* with different numbers of VCS or VCS-PO. It can be seen that *ROE* of the VCS-PO is greater than that of VCS under the same VCS number. When the VCS number is one, regardless of having P-O conversion or not, the system can achieve about 80% of the optimal results. In a majority of application scenarios, the system with SVCS is sufficient to meet the insulation requirements. As for a few cases with high requirements for the thermal insulation, the system with DVCS is recommended to further improve the insulation performance, which can reach nearly 90% of the best results. The benefits to the insulation system become limited if continuing to increase the VCS

Please cite this article as: Shi C et al., Performance analysis of vapor-cooled shield insulation integrated with para-ortho hydrogen conversion for liquid hydrogen tanks, International Journal of Hydrogen Energy, https://doi.org/10.1016/j.ijhydene.2022.10.154

Table 4 – Comparison of *ROE* with different numbers of VCS or VCS-PO.

Case	Heat leak q_0 (W/m^2)	Reduction of heat leak η (%)	*ROE* (%)
non-VCS	0.288	–	–
SVCS *vs.* SVCS-PO	0.112 *vs.* 0.099	61.1 *vs.* 65.6	76.5 *vs.* 80.1
DVCS *vs.* DVCS-PO	0.086 *vs.* 0.076	70.1 *vs.* 73.6	87.8 *vs.* 89.9
TVCS *vs.* TVCS-PO	0.081 *vs.* 0.068	71.9 *vs.* 76.4	90.1 *vs.* 93.3
AVCS *vs.* AVCS-PO	0.058 *vs.* 0.052	79.9 *vs.* 81.9	100 *vs.* 100

number to more than three, which is consistent with the conclusions of Ref. [14]. This work provides a guidance for the design of the high-performance thermal insulation system for liquid hydrogen tanks.

Conclusions

A thermodynamic model of the VDMLI with multi-VCS integrated with P-O conversion is established to investigate the impact of the VCS number and P-O conversion on the insulation performance. The main conclusions are as follows:

(1) The addition of VCS significantly affects the proportions of three heat transfer modes in the VDMLI. The proportion of radiation is greatly reduced, while those of solid heat conduction and gas heat conduction are increased. In addition, the temperature profile inside the VCS becomes flatter with the increases of the VCS number. Compared to that without VCS, the heat leak with multiple VCSs can be reduced by max. 79.9%.

(2) The heat leak with the SVCS-PO is 11.6% less than that of the SVCS. The heat taken away by the conversion heat plays a relatively greater role at the low-temperature region. The optimal position of the VCS-PO is closer to the tank wall compared to that of the VCS due to the combined effect arising from the addition of the VCS and P-O conversion. The temperature at the position where the VCS is added decreases from 128.6 K to 120.1 K after the P-O conversion is further added. In addition, the deterioration of the insulation performance has a linear relationship with the reduction of catalytic efficiency.

(3) A relative optimization efficiency (*ROE*) is proposed to evaluate the improvement of the VCS number on the thermal insulation performance visually. For the system with the SVCS and SVCS-PO, *ROE* can reach 76.5% and 80.1%, which is sufficient to meet a majority of insulation requirements. As for cases with higher requirements, the system of the DVCS and DVCS-PO is recommended to further improve the insulation performance with the *ROE* of 87.8% and 89.9%, respectively. The benefits to the insulation system are extremely trifling if the VCS number is increased to more than three.

Declaration of competing interest

The authors declare that they have no known competing financial interests or personal relationships that could have appeared to influence the work reported in this paper.

Acknowledgement

This work is financially supported by the National Key Research and Development Program of China (No. 2021YFB4000700) and the National Postdoctoral Program for Innovative Talents, China (BX2021253) .

REFERENCES

[1] Zhang F, Zhao P, Niu M, Maddy J. The survey of key technologies in hydrogen energy storage. Int J Hydrogen Energy 2016;41:14535–52. https://doi.org/10.1016/j.ijhydene.2016.05.293.

[2] da Silva Veras T, Mozer TS, da Costa Rubim Messeder dos Santos D, da Silva César A. Hydrogen: trends, production and characterization of the main process worldwide. Int J Hydrogen Energy 2017;42:2018. https://doi.org/10.1016/j.ijhydene.2016.08.219. –33.

[3] Abe JO, Popoola API, Ajenifuja E, Popoola OM. Hydrogen energy, economy and storage: review and recommendation. Int J Hydrogen Energy 2019;44:15072–86. https://doi.org/10.1016/j.ijhydene.2019.04.068.

[4] Liu Z, Li Y, Xie F, Zhou K. Thermal performance of foam/MLI for cryogenic liquid hydrogen tank during the ascent and on orbit period. Appl Therm Eng 2016;98:430–9. https://doi.org/10.1016/j.applthermaleng.2015.12.084.

[5] Hedayat A. Analytical modeling of variable density multilayer insulation for cryogenic storage. vol. 613. In: AIP Conference Proceedings. Madison, Wisconsin (USA): AIP; 2002. p. 1557–64. https://doi.org/10.1063/1.1472190.

[6] Hastings LJ, Hedayat A, Brown TM. Analytical modeling and test correlation of variable density multilayer insulation for cryogenic storage. 2004.

[7] Scott RB. Thermal design of large storage vessels for liquid hydrogen and helium. J Res Natl Bur Stan 1957;58:317. https://doi.org/10.6028/jres.058.038.

[8] Bejan A. A general variational principle for thermal insulation system design. Int J Heat Mass Tran 1979;22:219–28. https://doi.org/10.1016/0017-9310(79)90145-5.

[9] Cunnington GR. Thermodynamic optimization of a cryogenic storage system for minimum boiloff. 20th aerospace sciences meeting. 2012. https://doi.org/10.2514/6.1982-75.

[10] Chato JC, Khodadadi JM. Optimization of cooled shields in insulations. J Heat Tran 1984;106:871–5. https://doi.org/10.1115/1.3246766.

[11] Kim SY, Kang BH. Thermal design analysis of a liquid hydrogen vessel. Int J Hydrogen Energy 2000;25:133–41. https://doi.org/10.1016/S0360-3199(99)00020-8.

[12] Babac G, Sisman A, Cimen T. Two-dimensional thermal analysis of liquid hydrogen tank insulation. Int J Hydrogen Energy 2009;34:6357–63. https://doi.org/10.1016/j.ijhydene.2009.05.052.

Please cite this article as: Shi C et al., Performance analysis of vapor-cooled shield insulation integrated with para-ortho hydrogen conversion for liquid hydrogen tanks, International Journal of Hydrogen Energy, https://doi.org/10.1016/j.ijhydene.2022.10.154

[13] Jiang WB, Zuo ZQ, Huang YH, Wang B, Sun PJ, Li P. Coupling optimization of composite insulation and vapor-cooled shield for on-orbit cryogenic storage tank. Cryogenics 2018;96:90–8. https://doi.org/10.1016/j.cryogenics.2018.10.008.
[14] Zheng J, Chen L, Wang J, Zhou Y, Wang J. Thermodynamic modelling and optimization of self-evaporation vapor cooled shield for liquid hydrogen storage tank. Energy Convers Manag 2019;184:74–82. https://doi.org/10.1016/j.enconman.2018.12.053.
[15] Petitpas G, Aceves SM, Matthews MJ, Smith JR. Para-H2 to ortho-H2 conversion in a full-scale automotive cryogenic pressurized hydrogen storage up to 345 bar. Int J Hydrogen Energy 2014;39:6533–47. https://doi.org/10.1016/j.ijhydene.2014.01.205.
[16] Wilhelmsen Ø, Berstad D, Aasen A, Nekså P, Skaugen G. Reducing the exergy destruction in the cryogenic heat exchangers of hydrogen liquefaction processes. Int J Hydrogen Energy 2018;43:5033–47. https://doi.org/10.1016/j.ijhydene.2018.01.094.
[17] Donaubauer PJ, Cardella U, Decker L, Klein H. Kinetics and heat exchanger design for catalytic ortho-para hydrogen conversion during liquefaction. Chem Eng Technol 2019;42:669–79. https://doi.org/10.1002/ceat.201800345.
[18] Park J, Lim H, Rhee GH, Karng SW. Catalyst filled heat exchanger for hydrogen liquefaction. Int J Heat Mass Tran 2021;170:121007. https://doi.org/10.1016/j.ijheatmasstransfer.2021.121007.
[19] Xu P, Lei G, Xu Y, Wen J, Wang S, Li Y. Study on continuous cooling process coupled with ortho-para hydrogen conversion in plate-fin heat exchanger filled with catalyst. Int J Hydrogen Energy 2022;47:4690–703. https://doi.org/10.1016/j.ijhydene.2021.11.074.
[20] Nast TC. Investigation of a para-ortho hydrogen reactor for application to spacecraft sensor cooling. 1983.
[21] Bliesner RM, Leachman JW, Adam PM. Parahydrogen–orthohydrogen conversion for enhanced vapor-cooled shielding of liquid oxygen tanks. J Thermophys Heat Tran 2014;28:717–23. https://doi.org/10.2514/1.T4366.
[22] Pedrow BP, Muniyal Krishna SK, Shoemake ED, Leachman JW, Matveev KI. Parahydrogen–orthohydrogen conversion on catalyst-loaded scrim for vapor-cooled shielding of cryogenic storage vessels. J Thermophys Heat Tran 2021;35:142–51. https://doi.org/10.2514/1.T5136.
[23] Wang L, Ye S, Li Y, Yan T, Xue L. Analysis on cold energy release schemes in para-ortho hydrogen conversion and its utilization potential in space. Journal of Astronautics 2019;40:109–17. https://doi.org/10.3873/j.issn.1000-1328.2019.01.013. 01 [in Chinese].
[24] Martin JJ, Hastings L. Large-scale liquid hydrogen testing of variable density multilayer insulation with a foam substrate. 2001.
[25] Zheng J, Chen L, Wang J, Xi X, Zhu H, Zhou Y, et al. Thermodynamic analysis and comparison of four insulation schemes for liquid hydrogen storage tank. Energy Convers Manag 2019;186:526–34. https://doi.org/10.1016/j.enconman.2018.12.053.
[26] Yin L, Ju Y. Process optimization and analysis of a novel hydrogen liquefaction cycle. Int J Refrig 2020;110:219–30. https://doi.org/10.1016/j.ijrefrig.2019.11.004.
[27] McIntosh GE. Layer by layer MLI calculation using a separated mode equation. In: Kittel P, editor. Advances in Cryogenic Engineering. Boston, MA: Springer US; 1994. p. 1683–90. https://doi.org/10.1007/978-1-4615-2522-6_206.
[28] Keller CW, Cunnington GR, Glassford AP. Thermal performance of multilayer insulations. 1974.
[29] Barron RF, Nellis GF. Cryogenic heat transfer. CRC Press; 2017.
[30] Yu J, Zhang Q, Kang H, et al. Comprehensive optimization design of VCS composite thermal insulation structure for cryogenic propellant tank. Vacuum and Cryogenics 2021;27(2):165–70. https://doi.org/10.3969/j.issn.1006-7086.2021.02.010 [in Chinese].
[31] Corruccini RJ. Gaseous heat conduction at low pressures and temperatures. Vacuum 1959;7(8):19–29. https://doi.org/10.1016/0042-207X(59)90766-3.
[32] Wang B, Huang YH, Li P, Sun PJ, Chen ZC, Wu JY. Optimization of variable density multilayer insulation for cryogenic application and experimental validation. Cryogenics 2016;80:154–63. https://doi.org/10.1016/j.cryogenics.2016.10.006.
[33] Huang Y, Wang B, Zhou S, Wu J, Lei G, Li P, et al. Modeling and experimental study on combination of foam and variable density multilayer insulation for cryogen storage. Energy 2017;123:487–98. https://doi.org/10.1016/j.energy.2017.01.147.
[34] Chen L, Xiao R, Cheng C, Tian G, Chen S, Hou Y. Thermodynamic analysis of the para-to-ortho hydrogen conversion in cryo-compressed hydrogen vessels for automotive applications. Int J Hydrogen Energy 2020;45:24928–37. https://doi.org/10.1016/j.ijhydene.2020.05.252.

Please cite this article as: Shi C et al., Performance analysis of vapor-cooled shield insulation integrated with para-ortho hydrogen conversion for liquid hydrogen tanks, International Journal of Hydrogen Energy, https://doi.org/10.1016/j.ijhydene.2022.10.154